



Meltwater Storage in the firn of Kaskawulsh Glacier, Yukon Territory, Canada

Naomi Ochwat¹, Shawn Marshall^{1,2}, Brian Moorman¹, Alison Criscitiello,³ Luke Copland⁴

¹Department of Geography, University of Calgary, Calgary, Alberta, T2N 1N4, Canada

5 ²Environment and Climate Change Canada, Gatineau, Quebec, K1A 0H3, Canada

³Department of Earth and Atmospheric Sciences, University of Alberta, Edmonton, T6G 2R3, Canada

⁴Department of Geography, Environment and Geomatics, University of Ottawa, Ottawa, Ontario K1N 6N5, Canada

Correspondence to: Naomi Ochwat (naomi.ochwat@ucalgary.ca)

10 **Abstract.** In recent years, the analysis of firn in Greenland, Svalbard, and other high Arctic regions has contributed to the
understanding of meltwater retention in firn and its importance to measurements of glacier mass balance. This has provided
insight into firn densification processes and meltwater retention. Changes in these attributes can also provide insight into
meteorological variability and climate trends. In spring 2018, two firn cores (21 m and 36 m in length) were extracted from
the accumulation zone of Kaskawulsh Glacier, St. Elias Mountains, Yukon. The cores were analyzed for ice layer
15 stratigraphy, density, and glaciochemical time series (oxygen isotopes and major ions). Meltwater percolation and refreezing
events were evident in the cores. The quantity of ice layers, the presence of liquid water at 34.5 m depth, interpreted as a
perennial firn aquifer (PFA), and the altered isotopic and glaciochemical signature all indicate this process. This melt
resulted in an estimated surface lowering of 10 ± 0.8 cm/yr between 2005 and 2018. The information gleaned from
Kaskawulsh Glacier supports the need for improved and field-validated density assumptions for geodetic mass balance
20 methods.

1 Introduction

With the increasing affects of climate change and the need for understanding glacier and ice sheet melt rates, geodetic
methods are useful for indirect measurements of mass balance. Based on repeat altimetry, geodetic approaches to mass
25 balance monitoring rely on several assumptions. Estimates must be made of the density of snow, firn, and ice at the sampling
location, with the additional assumption that these densities remain unchanged between the two measurement dates. With
large changes in elevation that can occur over decadal timescales, changes in density of the firn may have little impact on the
mass balance calculations from geodetic measurements (Moholdt et al., 2010a). However, over shorter time periods (years),
this may not be true (Moholdt et al., 2010b). Meltwater percolation and refreezing can significantly change the firn density
30 profile and density of the accumulation zone of a glacier (Gascon et al., 2013). These modifications of firn density can
introduce large uncertainties when using geodetic techniques to determine glacier mass balance. For example, Moholdt et al.
(2010a) determined mass balance on a Svalbard glacier to be -4.3 ± 1.4 Gt/yr, with the large uncertainty attributed to limited



35 knowledge of the snow and firn density and their spatial and temporal variation. By altering the density and causing surface lowering, meltwater percolation, refreezing, and liquid water storage all complicate the interpretation of geodetic mass balance data.

40 Warming firn can result in increased meltwater production and altered firn densification processes. Initially, melt can round the snow grains and increase the snowpack density. If the surface continues to melt, the meltwater can percolate into the firn and refreeze as ice layers or lenses. On temperate glaciers, meltwater that percolates below the winter cold layer often will not refreeze, and may thus form a firn aquifer (Munneke et al., 2014). These internal accumulation processes can significantly affect the density of the firn. Once ice layers or firn aquifers form, this also effects how meltwater percolates through the firn thereafter. Due to the spatial heterogeneity of meltwater retention, percolation, and refreezing processes, there are still many gaps in knowledge on how to model these processes and subsequently estimate firn density in areas where these processes occur (van As et al., 2016).

45

Meltwater retention in firn is also important for estimating glacial runoff contributions to sea level rise. Recently, there have been extensive studies investigating the meltwater and refreezing occurring in southern Greenland (Humphrey et al., 2012; Harper et al., 2012; De La Peña et al., 2015; Macferrin et al., 2019), Arctic Canada (Bezeau et al., 2013; Gascon et al., 2013), and Svalbard (Christianson et al., 2015). Using ground and airborne radar as well as ice cores, researchers have estimated the volume of water storage in the percolation zone of the Greenland Ice Sheet and have investigated the interactions of the meltwater and ice and their subsequent effects on hydrology and run-off mechanisms (e.g., Harper et al., 2012; Koenig et al., 2014; Machguth et al., 2016). Increased melt rates in the Greenland percolation zone may lead to the expansion of low-permeability ice layers, causing run-off in Greenland to increase and expediting the movement of water from the ice sheet to the ocean (Macferrin et al., 2019). These processes are not limited to the Arctic; it is necessary to investigate these properties on mountain glaciers as well, for improved estimates and models of glacier mass balance and associated sea-level rise.

60 In this study two firn cores were retrieved on Kaskawulsh Glacier, St. Elias Icefields, Yukon, Canada. The firn cores were analyzed for density and the effects of meltwater percolation and refreezing. This included physical descriptions and quantification of ice layers and lenses, as well as analyses of the stable isotopes $\delta^{18}\text{O}$ and δD and major ions. Foy et al., (2011) recorded density up to 8.1m depth in 2007 in the accumulation zone of Kaskawulsh Glacier. However, recent and detailed documentation of firn density in the St. Elias Icefields is lacking. The region was also the location of numerous pioneering glaciological studies in the 1960s, documented in a series of Icefield Ranges Research Reports (e.g., IRRP 1963, 1965, 1972). These early studies provide an estimate of firn density within the upper 15 m from a core close to our drilling site, providing an estimate of changes over the past ~50 years.

65



2 Methods

2.1 Study Area

We retrieved two firn cores in May 2018 from the upper accumulation zone of Kaskawulsh Glacier in the St. Elias Mountains (Figure 1), near the icefield divide. The St. Elias Mountains are located in the southwest corner of Yukon Territory, Canada (Figure 1). The peaks in this mountain range are predominantly between 300 – 2200 m above sea level (a.s.l.), with several notable exceptions of mountains higher than 3200 m, including Mount Logan at 5959 m a.s.l. (Foy et al., 2011). The St. Elias range is home to the largest icefield outside of the polar regions, with an area of 46,000 km² (Berthier et al., 2010). Like most high northern latitudes, Yukon Territory is warming (Foy et al., 2011; Williamson et al., 2020) and there is a need to better understand and document the impacts of climate change on the St. Elias Icefield.

75

Kaskawulsh Glacier is a large temperate valley glacier located on the eastern side of the St. Elias Mountains within the Donjek Range, and is approximately 70 km long and 3 – 4 km wide. The drill site is located on the upper north arm of the glacier in the accumulation zone (60.78°N, 139.63°W), at an elevation of ~2640 m a.s.l. Previous studies at Kaskawulsh Glacier include an analysis of volume change over time using satellite imagery (Foy et al., 2011). There were also several reports in the early 1960s that documented various glaciological characteristics and processes occurring in the St. Elias Mountains (Grew and Mellor, 1966; Wood, 1963). A weather station (Copland Weather Station, Figure 1) is 12 km southwest of the drill site (60.70°N, 139.80°W, 2600 m a.s.l.) has been in service since 2013 (Williamson et al., 2020). The temperature sensor is an Onset S-THB-M002 with an accuracy of $\pm 0.2^\circ$ C, mounted inside an Onset RS3 naturally vented solar radiation shield. There was a recent expedition (June 2018) at a nearby location, Kreutz Drill Site (Figure 1) (Kreutz, personal comm.) Other studies in the region include analysis of ice cores from the Eclipse Icefield, located 12 km northwest of our drill site (e.g., Zdanowicz et al., 2014 and Yalcin et al., 2006).

80
85

2.2 Field Methods

Two 8-cm diameter cores were drilled using an ECLIPSE ice core drill (Icefield Instruments, Yukon Territory, Canada). The seasonal snow had a depth of 4.4 m. With a starting depth of 2 m below the snow surface, Core 1 was 34.6 m long and reached a depth of 36.6 m, and Core 2 was 19.5 m long and reached a depth of 21.5 m. The two cores were drilled 60 cm apart, and core stratigraphy and density were recorded in the field. At a depth of 34.5 m during the drilling of Core 1, liquid water became evident; drilling was stopped at a depth of 36.6 m to avoid the risk of the drill freezing in the hole. A complementary 1 m deep snow pit was dug several meters away, allowing for detailed surface density measurements and sample collection for chemical and isotopic analysis.

90
95

Once the cores were retrieved, the presence of ice layers, lenses and melt-affected firn was logged and the stratigraphic character, depth, and thickness were recorded. When an ice horizon extended across the entire width of the core, it was



labeled as an ice layer. If the ice horizon was of more limited lateral extent, it was labeled an ice lens. Ice lenses were occasionally wedge shaped. Other types of melt-affected firn were identified by the lack of grain boundaries and the presence of air bubbles. Other noticeable features were also documented (e.g., the texture and visual appearance of the firn, such as opacity, which may have indicated melt-affected firn). Each core section was then sawed into 10-cm long sections. Each 10-cm section had its diameter measured at each end and was bagged, weighed, and assessed for the quality of the core sample and its cylindrical completeness (f). The average diameter was used to determine the volume of the core section (V). Together with the mass of the core section, m , density was calculated:

$$\rho = m/V, \text{ with } V = f\pi L(D/2)^2 \quad (1)$$

Where ρ is the density of the firn, D is the average core section diameter, L is the length, and f is the subjectively assessed fraction of completeness of the core section. For instance, if visual inspection indicated that about 5% of the core was missing (e.g., due to missing ice chips from the core dogs of the drill head), then f would be 0.95. Outliers were removed if they were not physically possible (e.g., values $>917 \text{ kg/m}^3$ or $<300 \text{ kg/m}^3$ at depths greater than 4 m). The ice cores were transported back to Kluane Lake Research Station frozen, where the individual sub-samples were melted at ambient temperature in sample bags. Samples were then transferred into 20-ml high-density polyethylene (HDPE) vials; no headspace was allowed in the HDPE vials, and HDPE caps were sealed with parafilm. The 20-ml samples were transported in a cooler ($\sim 4^\circ\text{C}$) to Alberta for chemical analysis. During transport and melting, some Core 2 sample bags were damaged, such that the density could not be calculated on all Core 2 samples.

2.3 Analysis Methods

2.3.1 Density Analysis

In order to calculate the uncertainty of the density calculations, numerous sources of error were assessed using standard error analysis. Random and human error were taken into account and propagated through the equations. The uncertainty in f is difficult to assign, but is the largest source of uncertainty in the density calculations. Three different people performed this evaluation with occasional inter-comparison of values and therefore there is subjectivity in the f values. To be conservative, the following uncertainties were assigned for f :

$$\begin{aligned} &\pm 0.2 \text{ for } f \leq 0.8, \\ &\pm 0.1 \text{ for } f \geq 0.9 \end{aligned}$$

The uncertainty of a higher f value is lower because it is more obvious when a core is of good quality; less complete cylinders are more difficult to assess, hence the greater uncertainty for values of $f \leq 0.8$. Here, an upper density bound of



130 917 kg/m³ (the density of pure ice) was assigned if the calculated density was larger than physically possible. The f values for Core 2 were not recorded in the field. The average core quality value of Core 1 was used for Core 2, given the likelihood that the overall quality of the cores would be similar due to their very close proximity.

Ice content (i.e. ice fraction), F_i , was calculated for each 10-cm section of the firn core. Here ice was defined based on its
135 lack of air bubbles and crystalline structure, as compared to granular structure. Ice content was calculated instead of melt percent, as melt percent generally assumes the meltwater remains within the net annual accumulation layer, which cannot be assumed here. The thickness of individual ice layers was summed within each 10-cm core section. On average, the ice lenses were observed to occupy 50% of the core samples; therefore their thickness was divided by two before being summed. For each core section, total ice content was divided by the length of the section, L , to give F_i .

140

To understand the firn densification process in the absence of refrozen meltwater, the ‘background’ firn density is of interest. For each sample, we estimate this by subtracting the mass and volume of the ice to give the firn density in the absence of ice content. We use a 30-cm moving average of ice content and density in order to smooth out a possible deviation of ± 10 cm in assigning the location of the ice features within the stratigraphy. Here, ice layers and lenses were assumed to have a density
145 of 874 kg/m³, based on the average density of firn-core sections that were 100% ice in Greenland (873 kg/m³) and Devon Ice Cap (875 kg/m³) (Machguth et al., 2016; Bezeau et al., 2013). This is different than the 917 kg/m³ upper bound used in the outlier analysis because that is the theoretical limit for pure ice, whereas this density has been determined using measured data from two other sites as well and incorporates the fact that the observed ice layers and lenses had tiny bubbles in them, indicating they were not pure ice. Each sample has a measured bulk density, ρ_b , which we assume to result from a binary
150 mixture of ice and firn, with densities ρ_f and ρ_i . Ice and firn fractions, F_i and F_f , were defined with $F_i + F_f = 1$. The background firn density is then calculated following:

$$\rho_f = (\rho_b - \rho_i F_i) / F_f \quad (2)$$

In some cases there is no ice content ($F_i = 0$), so $\rho_f = \rho_b$. Surface lowering associated with refreezing was calculated for each core section using the background firn density, ρ_f , and length of the section, L . For each core sample, the ‘thinning’ or
155 surface lowering associated with the ice content, ΔL , can be estimated by reverting the ice to the density of the background firn, as follows:

$$\Delta L = L \left[\left(F_f + \frac{\rho_i F_i}{\rho_f} \right) - 1 \right] \quad (3)$$

This is summed for the whole core to give the full amount of surface lowering associated with meltwater percolation and refreezing.



160 2.3.2 Stable Isotope and Ion Analysis

At the University of Calgary Isotope Science Laboratory (ISL), the liquid samples were pipetted into 2 ml glass isotope vials with septa caps. Using a Los Gatos Research Liquid Water Isotope Analyzer, Enhanced Performance Model DLT-100, the samples were run with the standards: Vienna Standard Mean Ocean Water (VSMOW), Vienna Standard Light Antarctic Precipitation (VSLAP), and Greenland Ice Sheet Precipitation (GISP).

165

At the University of Alberta's Canadian Ice Core Lab (CICL), core samples were analyzed for anions and cations using a Dionex ICS-5000. The analysis included anions: MSA^- , Cl^- , Br^- , NO_3^{2-} , PO_4^{3-} ; and cations: Na^+ , Mg^{2+} , K^+ , Ca^{2+} , SO_4^{2-} , and NH_4^+ .

3 Results

170 3.1 Density

The first 4.4 m of both cores was observed to be snow. At a depth of 4.4 m there was significant ice crust, representing the 2017 summer melt surface. This surface snow layer was also dry. The 4.4 m of snow had an average density of $450 \pm 21 \text{ kg/m}^3$.

175 The overall pattern of density resembles a typical densification curve (Cuffey and Paterson, 2010). Even though there is large scatter in the density values and a large uncertainty associated with each point, the firn density versus depth shows a logarithmic increase, as to be expected given Sorge's Law of densification (Bader, 1954) (Figure 2). To highlight this, a logarithmic curve was fitted to the density data. The density rapidly increases in the first 5 m below the snow surface. Between 5 and 10 m depth the density varies widely, from 300 to 900 kg/m^3 . Below 10 m, firn density increases
180 logarithmically from approximately 550 to 750 kg/m^3 . This corresponds with the second phase of densification in Sorge's Law. Between 20 and 32 m depth there is a wide range of density values, from approximately 650 to 908 kg/m^3 . As a whole, Core 2 follows a similar pattern to Core 1, with an abrupt initial increase and then scattered values at greater depths.

For the specific calculations of firn density, we omit the upper 4.4 m of the core, which represented the seasonal snow
185 accumulation from winter 2017-2018. Below this, in the upper 10 m of firn, Cores 1 and 2 have average densities of $558 \pm 4 \text{ kg/m}^3$ and $571 \pm 3 \text{ kg/m}^3$ respectively, giving an overall average density of $564 \pm 2 \text{ kg/m}^3$. Using both cores to 21 m depth, the upper 17 m of Kaskawulsh firn has an average density of $608 \pm 2 \text{ kg/m}^3$. Core 1 extends to a depth of 36.6 m, representing ~ 32 m of firn with an average density of $670 \pm 2 \text{ kg/m}^3$. Based on the high densities and liquid water content in the bottom sections of the core, we believe $670 \pm 2 \text{ kg/m}^3$ provides an estimate of the average density of the upper 32.2 m of
190 firn.



Total ice content in Core 1 was 1.53 m or 1.34 m w.e. This is equivalent to 4.2% by volume (Table 1) and 5.8% by mass. Using Eq. 2 to calculate the ice content over the full depth range of Core 1, we estimate a background firn density of 660 ± 6 kg/m³, 4.3% less than the bulk density of the firn (Table 1). Core 2 had a similar average firn density and ice content to the upper 21 m of Core 1, representing 3.8% by volume.

The total water equivalent (w.e.) of Core 1 is calculated to be 23.22 m w.e. Using the average accumulation rate of the Icefield Ranges Research Reports, 1.76 m w.e./yr (Wagner, 1963; Holdsworth, 1965), Core 1 represents approximately 13 years of net accumulation, from 2005 to 2018.

200 3.2 Stratigraphy

The stratigraphy of Kaskawulsh Glacier firn cores indicates numerous ice layers and melt-affected firn. The first 6 m of the stratigraphy display several small ice layers (<2.5 cm thick), interpreted as wind crusts in the snow (Figure 3). Several thick (>10 cm) ice layers are found between 6 and 26 m depth. The largest ice layer in Core 1 was 22 cm thick, found at 14.1 m. At 26.4 m the ice layers and lenses disappeared. Below this the firn is almost entirely meltwater-affected, based on the appearance and texture of the firn, but is without the quantity of ice lens or layer content that was present in the first 25 m. We interpret this section of the core as infiltration ice: water-saturated firn that has experienced refreezing. At 30 m depth the meltwater effects were absent and there were two small ice layers and an ice lens. At 30.6 m the firn was melt-affected again. From 34.5 to 36.6 m the core sections retrieved expelled liquid water as the sections were extracted from the core barrel.

210

In Core 2 there were numerous ice layers starting at a depth of 3.8 m, and below 4.4 m the firn was meltwater-affected. There was a thick ice layer at 6.6 m that was 30 cm lower than a similar ice layer in Core 1 (at 6.3 m). There were numerous melt-affected layers between ice lenses much closer to the surface in Core 2. In Core 1 there were several ice layers at ~10 m depth, and these layers were not present in Core 2. At 14.4 m another section of the firn had numerous ice layers. This was also seen in Core 1 but is 20-30 cm deeper here. At 14.6 m the thickest ice layer was encountered (12 cm), corresponding well with the thickest layer in Core 1. Between 16 and 21.5 m the firn was melt-affected. The differences between Core 1 and Core 2 stratigraphy can be attributed to horizontal variability in meltwater infiltration causing heterogeneous spacing of ice layers and lenses. This is known to occur at length scales less than 1-m (Parry et al., 2007; Harper et al., 2011).

3.3 Stable Isotopes

220 The range of $\delta^{18}\text{O}$ values in the winter 2017-2018 snowpack was -19.5 to -29% . Since these samples were acquired before the onset of summer melt, this is assumed to reflect depositional values for fall through spring precipitation at this site, with no evidence for post-depositional modification. Below the seasonal snowpack, stable isotope variations in the firn are largely



washed out. No summer peaks are preserved (i.e., values greater than -22%), and most of the winter peaks are also washed out. Several negative peaks are partially preserved, indicated by red arrows in Figure 4. In Core 1 (Figure 4) the average $\delta^{18}\text{O}$ for the 36.6-m core is $-24.6 \pm 0.7\%$. There are several periods of homogenization where the variability is less than $\sim 2\%$. Between 26.9 and 31.9 m the range is -24.8 to -23.2% with an average of -23.9% , but below this the $\delta^{18}\text{O}$ values begin to decrease linearly. The bottom part of the core has a range of -25.9 to -23.3% and an average of -24.8% . Please note that all of the major ion data were so severely washed out that the time series are not presented here; these data were not useful for analyses, but also testify to complete flushing of the firn to 36-m depth.

230 4 Discussion

4.1 Meltwater percolation and refreezing effects

Kaskawulsh Glacier has indications of widespread meltwater percolation and refreezing. This is evident in the washout of the isotopic signal. Meltwater is stored within the firn as ice, as indicated by the presence of ice layers and infiltration ice. It is also being stored in liquid form as a perennial firn aquifer (PFA). The water at depth is at least one year old, and likely the accumulation of numerous melt seasons; drilling occurred in May, prior to the onset of spring melt and any potential summer replenishment of the aquifer. The solid and liquid phase storage mechanisms in the Kaskawulsh Glacier firn layer have different implications for the mass balance of the glacier. Liquid water is commonly found in the temperate firn of low- and mid- latitude mountain glaciers and has played an important role in meltwater storage and glacier hydrology (Fountain and Walder, 1989; Scheider, 1999). Depending on the melt, firn aquifer thickness, and temperature of the firn, the storage of liquid water at the firn-ice interface delays runoff from hours to weeks or longer (Jansson et al., 2003) and can account for as much as 64% of internal accumulation, as found in Alaska and Sweden (Schneider, 1999; Trabant and Mayo, 1985).

The water in the firn aquifer on Kaskawulsh Glacier is likely to be flowing, redistributing mass. The drill site was located high in the glacier's accumulation zone, with a gently sloping surface ($<0.6^\circ$) resulting in a subtle hydraulic gradient. The low concentration of mobile ions in the saturated firn also implies that ions are being transported away from the site. If they were remaining within the firn column, there would likely be greater ion concentrations near the bottom of the core. We likely drilled into the top of the water table of the firn aquifer. There may be flow along the firn-ice interface down slope, as well as possible Darcian flow within the firn aquifer itself. It may also enter the englacial hydrological system and eventually reach the bed of the glacier; for example research on Storglaciären showed that there might be a subglacial aquifer fed from the firn area (Jansson et al., 2003).

The liquid-phase meltwater retention on Kaskawulsh is similar to the firn aquifers found in the high-accumulation areas of southern Greenland and Svalbard (e.g., Miège et al., 2016; Christianson et al., 2015) and different than the water-saturated



layers commonly found on temperate glaciers. Firn aquifers that have been studied on temperate mountain glaciers typically
255 have a saturated layer close to the surface (for example, 5 m below the surface at Storglaciären), have active discharge and
recharge processes (Fountain and Walder, 1998; Schneider, 1999), and appear to experience seasonal drainage over the
winter months (Fountain, 1989, 1996; Jansson et al., 2003), likely due to high slope gradients. In 2012, “water-saturated”
firn was found at 40-m depth in an ice core from Mt. Waddington, British Columbia (Neff et al., 2012). However, they
reported no significant alteration of chemistry from the melt above this layer and no additional analysis of this layer was
260 discussed (Neff et al., 2012). In 2015, a PFA was found on Holtedahlfonna icefield in Northwest Svalbard (Christianson et
al., 2015), and in 2019 a PFA at Lomonosovfonna ice field on Svalbard was investigated (Hawrylak and Nilsson, 2019).
According to Pohjola et al. (2002), Lomonosovfonna has high amounts of melt, enough to alter the stable isotopes and
chemistry of an ice core taken in 1997, yet it was all refrozen within the annual accumulation layer. Now, 20 years later it is
known that there is a PFA on the same icefield (Hawrylak and Nilsson, 2019). Apart from these studies, there have been no
265 other published reports of PFAs on mountain glaciers (Christianson et al, 2015).

According to Munneke et al. (2014), firn aquifer formation in Greenland is contingent upon a high amount of accumulation,
which helps to insulate the underlying firn from the winter cold wave. Mean annual temperatures in Greenland are well
below 0°C and firn aquifers require: (i) latent heat release from meltwater refreezing, to warm the snow and firn to 0°C,
270 along with (ii) meltwater penetration to depths of 10 m or more, to evade the winter cold wave (Munneke et al., 2014). Using
the partially preserved section of firn and earlier reports from the IRRP (Grew and Mellor, 1966; Wood, 1963), the estimated
accumulation rate at our core site on Kaskawulsh is 1.8 m w.e. per year. This is similar to reported accumulation rates where
PFAs have been identified in southeastern Greenland (e.g., Miège et al., 2016).

275 Temperature records from the previously mentioned weather station 12 km southwest of our core site (Figure 1) at 2600 m
a.s.l provide data for summer positive degree days (PDD), which can be taken as a proxy for summer melt extent (Table 2),
using the standard approach (Cuffey and Paterson, 2010). These data indicate that there was ample melting every summer
from 2014-2018, but with considerable interannual variability. Temperatures in summer 2015 were the warmest of the period
2014-2018, and it is possible that there was deep meltwater penetration and aquifer formation or recharge during that
280 summer. However, we do not know how old the deep aquifer is, or if it experiences annual recharge. It is possible that all of
the meltwater refreezes near the surface in cool summers (e.g., 2014), and deep percolation only occurs in years with high
amounts of melt (e.g., 2015, 2018).

4.2 Density of the upper Kaskawulsh Glacier

In the upper accumulation zone of Kaskawulsh Glacier the density of the upper ~17 m of firn has an average value of $608 \pm$
285 2 kg/m^3 in our two cores. The firn extends down at least 36 m from the snow surface, and potentially continues to further
depths, giving firn depths of at least 32 m. The average firn density over the full 32 m of the core was $670 \pm 2 \text{ kg/m}^3$. In



2007, Foy (2009) measured the average density of the first 8 meters as 510 kg/m^3 with a standard deviation of 110 kg/m^3 , although this estimate includes some snow. Grew and Mellor (1966) discuss a 15-m core (including snow) that was retrieved at IRRP Divide Camp A. The first 15 m are much less dense than the data we collected, with an estimated average density of roughly 500 kg/m^3 . Their firn densities do not reach 600 kg/m^3 until depths of more than 11 m, while we recorded values in excess of 600 kg/m^3 within the first 5 m. This also implies limited ice content in the IRRP core. One notable ice lens and one ice gland were reported in the Grew and Mellor study (1966). This study also suggests that there may be an indication of meltwater percolation into previous years' accumulation. A recent study identifies the St. Elias Mountains as a region that has warmed in recent decades (Williamson et al., 2020). A downscaled North American Regional Reanalysis (NARR) temperature dataset validated against regional meteorological data from 1979–2016, and shows a warming temperature trend of $0.021 \pm 0.012 \text{ }^\circ\text{C a}^{-1}$ for elevations between 2500–3000 m (Williamson et al., 2020). This amounts to a warming of roughly 1.2°C at our study site since the 1960s, which would increase the quantity of meltwater, refrozen ice, and melt-affected firn, increasing the density of firn in the St. Elias Mountains.

A range of values for firn density has been reported for alpine glaciers, with considerable variability (Table 3). Kaskawulsh Glacier firn is similar to the firn reported in Arctic Canada of 560 kg/m^3 (Zdanowicz et al., 2012) and that of Patagonia (Matsuoka and Naruse, 1999; Shiraiwa et al., 2002). It is more dense than the firn of Svalbard (Pälli et al., 2002; Nuth et al., 2010), but less dense than firn reported from the European Alps and the Himalayas (Table 3). The lower latitude glaciers are likely experiencing a substantial amount of meltwater percolation and refreezing, making ice layers more prevalent than the firn itself. The glaciers in central Svalbard have a different accumulation regime and may have a lower density snow to start with, due to the cold temperatures and low precipitation (depending on the location) (Pälli et al., 2002; Nuth et al., 2010; Eckerstorfer and Christiansen, 2011). Kaskawulsh Glacier firn is similar to the firn at other high latitudes that have not begun to melt significantly, yet.

4.3 Implications for geodetic mass balance

The effects of meltwater storage through refreezing or liquid retention on high mountain glaciers will complicate mass balance measurements. Geodetic mass balance measurements are compromised by climate change-induced densification that causes surface lowering of the accumulation zone (Reeh, 2008; Huss, 2013). Mass balance studies in Greenland indicate that changing melt regimes and the subsequent meltwater storage and unknown density of snow and firn pose the greatest uncertainty when modeling the mass balance of large ice sheets (Lenaerts et al., 2019). Research in Greenland proposes that ice-layer formation and the presence of firn aquifers may delay surface run-off until a certain amount of ice layers are present. If ice becomes too extensive, it can form an impermeable barrier that leads to enhanced surface runoff (MacFerrin et al., 2019). These phenomena and effects are not limited to Greenland and the high Arctic. This study demonstrates that Kaskawulsh Glacier also experiences meltwater storage in the form of ice layers and liquid water retention. The firn



stratigraphy found on Kaskawulsh Glacier is similar to high accumulation Arctic regions (Pohjola et al., 2002; De La Peña et al., 2012; Bezeau et al., 2013).
320

The accumulation zone of Kaskawulsh Glacier is estimated to have experienced 1.3 ± 0.8 m of surface lowering due to internal refreezing over the period represented by Core 1, which we estimate to be 13 years. This is a conservative estimate, because neither the meltwater retention due to the infiltration ice nor the presence of the firn aquifer is included in this estimate. Firn that is affected by these processes will be denser, with greater surface lowering associated with firn densification, and no change in mass only change in volume. Assuming 13 years of net accumulation (between 2005 and 2018) represented by Core 1, the average thinning rate due to ice-layer formation is 0.10 m/yr, approximately 2% of annual net accumulation. We suspect that the result is representative of the upper accumulation area of Kaskawulsh Glacier and divide region, an area of $\sim 81 \pm 12$ km² or 10% of the accumulation zone area (811 km²; Foy et al., 2011). Additional data is needed to assess the regional applicability, however given that temperature is the primary control on meltwater extent and refreezing (Samimi and Marshall, 2017; Humphrey et al., 2012; Parry et al., 2007), this may be broadly representative of the upper accumulation and Divide region.
325
330

Previous research has focused on elevation changes on Kaskawulsh Glacier in recent decades. Foy et al., (2011) found that the accumulation zone thinned by an average of 0.04-0.11 m/yr from 1977-2007: a total thinning of 1–3 m over this period. In Larsen et al. (2015) the mean elevation change profile of Kaskawulsh Glacier showed between 0-1 m/yr of negative elevation change towards the head of the glacier from 1995-2000. The thinning signal due to meltwater percolation and refreezing is within Foy et al.'s and Larsen et al.'s estimate, suggesting that some or all of the reported lowering could be due to mass redistribution and not mass loss.
335

Over long periods this may be insignificant due to the natural variability in the system and the uncertainties associated with the estimates. For example, Bamber and Riveria (2007) suggest that if the surface lowering due to densification is on the order of centimeters per year then it will not significantly affect geodetic mass balance techniques, but if it is larger then it needs to be taken into consideration if the time period is less than a decade. Additionally, data on short time periods (tens of years or less) may be skewed if there are a few years of significant surface lowering (Huss, 2013; Schneider and Jansson, 2004), or if there is a large seasonal variation in glacier surface height, such as southeast Alaska (Pelto et al., 2013). Therefore, the magnitude of surface lowering and the time period of investigation need to be taken into consideration together. Huss (2013) concludes that the uncertainties in densities when converting to volume change can account for 2-15% of mass change. This indicates that there is a substantial need for in-situ density measurements of glacier firn around the world, so that glacier mass balance can be accurately assessed. Estimates of the firn density of Kaskawulsh Glacier are important for geodetic mass balance measurements in the St. Elias region.
340
345
350



5 Conclusion

The upper accumulation zone of Kaskawulsh Glacier is experiencing meltwater percolation and refreezing, thus altering the density and causing the glacier surface to lower. The density of the first 32 m of firn is $670 \pm 1.6 \text{ kg/m}^3$, and firn densification due to meltwater refreezing into ice layers over the last ~13 years (2005-2018) is responsible for an estimated surface lowering of $10 \pm 8 \text{ cm/yr}$. In addition to meltwater retention as ice layers, we found liquid water below 34 m, interpreted as a PFA.

This study advances the understanding of the density of firn in this region to better inform geodetic mass balance studies. The presence of the PFA coincides with findings in high Arctic regions with warming firn. As the climate changes, and with expected increases in temperature and changes in precipitation patterns, the effects of meltwater percolation and refreezing are expected to become more widespread in high-latitude and high-altitude glaciers. The St. Elias Mountains are home to several large valley glaciers (>40 km in length) and several icefields (e.g., Bagley, St. Elias). Mass balance studies are needed for these glaciers and icefields to assess their contribution to sea level rise and changing downstream hydrological conditions, but their size necessitates geodetic approaches for this research. An estimation of the density of firn in this area will aid in geodetic mass balance studies. With one side of the mountain range experiencing a maritime climate and the other side a continental climate, it is essential to consider firn densification processes and the effect of meltwater percolation and refreezing. The firn characteristics at Kaskawulsh Glacier are likely representative of many melt-affected glaciers in such environments.

The Kaskawulsh Glacier PFA needs to be more widely studied. The spatial extent and depth of the aquifer is not yet known. Ground penetrating radar may be a method to investigate the spatial extent of the feature. Use of an electrothermal drill that can drill through water-saturated firn may allow estimations of the depth of the firn aquifer as well as subsequent studies on the potential flow of the water within the aquifer. This region will likely continue to experience increasing amounts of surface melt and refreezing within the snowpack and firn, therefore there is urgency to obtain climate records from this region.

Data availability. Datasets are being submitted to the Scholars Portal Dataverse. Inquiries can be directed to the corresponding author.

Author contribution. NO and AC collected field data. AC ran ion analyses, supervised the field campaign and helped with figures. SM contributed to the design, conception, and funding of the study. SM and BM provided supervision during the project. LC provided weather station data. NO analysed the data. NO wrote the manuscript, to which all co-authors contributed.



385

Competing interests. The authors declare no competing interests.

Acknowledgements. This work was part of the Polar Knowledge Canada Grant in support of Cryosphere-Climate Monitoring at Kluane Lake Research Station, Yukon Territory. We acknowledge the Natural Sciences and Engineering Research Council (NSERC) of Canada for additional financial support. We thank Parks Canada for permission to conduct this research
390 in Kluane National Park, under research and collection permit KLU-2018-28117. We are grateful for the field crew Étienne Gros and Peter Moraal, Icefield Instruments Inc. The Arctic Institute of North America, Kluane Lake Research Station, and Icefields Discovery supported fieldwork logistics. We thank Kristina Miller, University of Calgary, for field support and countless glaciological discussions, Shad O’Neel and Louis Sass of the U.S. Geological Survey for sharing firn density data
395 from Alaska, and Anne Myers of the Canadian Ice Core Laboratory for assistance in producing the major ion records.

References

- Ambach, W. and Eisner, H.: Analysis of a 20m firn pit on the Kesselwandferner (“Otztal Alps), J. Glaciol., 6, 223–231, 1966.
- Bader, H.: Sorge’s law of densification of snow on high polar glaciers, J. Glaciol., 2, 319–323, 1954.
- 400 Bamber, J. L. and Rivera, A.: A review of remote sensing methods for glacier mass balance determination. Global. Planet. Change, 59, 138–148, 2007.
- Berthier, E., Schiefer, E., Clarke, G. K. C., Menounos, B. and Rémy, F.: Contribution of Alaskan glaciers to sea-level rise derived from satellite imagery. Nat. Geosci. 3, 92–95, 2010.
- Bezeau, P., Sharp, M., Burgess, D. and Gascon, G.: Firn profile changes in response to extreme 21st-century melting at
405 Devon Ice Cap, Nunavut, Canada. J. Glaciol. 59, 981–991, 2013.
- Christianson, K., Kohler, J., Alley, R. B., Nuth, C. and Van Pelt, W. J. J.: Dynamic perennial firn aquifer on an Arctic glacier. Geophys. Res. Lett. 42, 1418–1426, 2015.
- Cuffey, K. M., and Paterson, W.: The Physics of Glaciers (4th ed.). Boston,: Elsevier. 1-683. 2010.
- De La Peña, S, I. M. Howat, P.W. Nienow, M. R. van den Broeke, E. Mosley-Thompson, S. F. Price, D. Mair, B. Noël, and
410 A. J. Sole.: Changes in the firn structure of the western Greenland Ice Sheet caused by recent warming. The Cryosphere, 9, 1203–1211, 2015.
- Eckerstorfer, M. and Christiansen, H. H.: The “High Arctic Maritime Snow Climate” in Central Svalbard. Arctic, Antarct. Alp. Res. 43, 11–21. 2011.
- Fountain, A. G.: Effect of Snow and Firn Hydrology on the Physical and Chemical Characteristics of Glacial Runoff.
415 Hydrol. Process. 10, 509–521, 1996.
- Fountain, A. G. and Walder, J. S.: Water flow through temperate glaciers. Rev. Geophys., 36, 299–328. 1998.



- Foy, N.: Changes in surface elevation and extent of the Kaskawulsh Glacier, Yukon Territory. (Published Master's Thesis), Department of Geography. University of Ottawa, Ottawa, Canada. 1-131, 2009.
- Foy, N., Copland, L., Zdanowicz, C., Demuth, M., Hopkinson, C.: Recent volume and area changes of Kaskawulsh
420 Glacier, Yukon, Canada. *J. Glaciol.*, 57, 515–525, <https://doi.org/10.3189/002214311796905596>, 2011.
- Gascon, G., Sharp, M., Burgess, D., Bezeau, P. and Bush, A. B. G.: Changes in accumulation-area firn stratigraphy and meltwater flow during a period of climate warming: Devon Ice Cap, Nunavut, Canada. *J. Geophys. Res. Earth Surf.* 118, 2380–2391, 2013.
- Grew, E., and Mellor, M.: High snowfields of the St. Elias Mountains, Yukon Territory, Canada. Hanover, N.H. U.S. Army
425 Materiel Command, Cold Regions Research & Engineering Laboratory Technical Report, 177, 1-26, 1966.
- Harper, J., Humphrey, N., Pfeffer, W. T., Brown, J., and Fettweis, X.: Greenland ice-sheet contribution to sea-level rise buffered by meltwater storage in firn. *Nature*, 491, 240–243, 2012.
- Harper, J., Humphrey, N., Pfeffer, T. and Brown, J.: Firn Stratigraphy and Temperature to 10 m Depth in the Percolation Zone of Western Greenland , 2007 – 2009. *Inst. Arct. Alp. Res.* 2007–2009. 2011.
- 430 Hawrylak, M., and Nilsson, E.: Spatial and Temporal Variations in a Perennial Firn Aquifer on Lomonosovfonna, Svalbard. Uppsala University Independent Project, 2019. <http://www.diva-portal.se/smash/get/diva2:1319193/FULLTEXT01.pdf>.
- He, Y., Yao, T., Theakstone, W., Cheng, G., Yang, M., and Chen, T.: Recent climatic significance of chemical signals in a shallow firn core from an alpine glacier in the South-Asia monsoon region, *J. Asian Earth Sci.*, 20, 289–296, 2002.
- Helsen, Humphrey, N. F., Harper, J. T., and Pfeffer, W. T.: Thermal tracking of meltwater retention in Greenland's accumulation
435 area. *J. Geophys. Res.*, 117, F01010, <https://doi.org/10.1029/2011JF002083>, 2012.
- Huss, M.: Density assumptions for converting geodetic glacier volume change to mass change, *The Cryosphere*, 7, 219–244. 2013.
- Jansson, P., Hock, R. and Schneider, T.: The concept of glacier storage: A review. *J. Hydrol.*, 282, 116–129, 2003.
- Koenig, L. S., Miège, C., Forster, R. R. and Brucker, L.: Initial in situ measurements of perennial meltwater storage in the
440 Greenland firn aquifer. *Geophys. Res. Lett.* 41, 81–85, 2014.
- Kreutz, K. J., Aizen, V. B., Dewayne Cecil, L., and Wake, C. P.: Oxygen isotopic and soluble ionic composition of a shallow firn core, Inilchek glacier, central Tien Shan, *J. Glaciol.*, 47, 548–554, 2001.
- Larsen, C. F., Burgess, E., Arendt, A. A., O'Neel, S., Johnson, A. J., and Kienholz, C.: Surface melt dominates Alaska glacier mass balance. *Geophys. Res. Lett.* 42, 5902–5908. <https://doi.org/10.1002/2015GL064349>, 2015.
- 445 Lenaerts, J. T. M., Medley, B., van den Broeke, M. R. and Wouters, B.: Observing and Modeling Ice Sheet Surface Mass Balance. *Rev. Geophys.* 57, 376–420, <https://doi.org/10.1029/2018RG000622>, 2019.
- Machguth, H., Eisen, O., Paul, F. and Hoelzle, M.: Strong spatial variability of snow accumulation observed with helicopter-borne GPR on two adjacent Alpine glaciers. *Geophys. Res. Lett.* 33, 1–5, 2006.



- MacFerrin, M. Machguth H, van As, D. C. Charalampidis, C., C. M. Stevens, C.M., Heilig, A., Vandecrux, B., P. L. Langen,
450 P. L., Mottram, R., Fettweis, X., van den Broeke, M. R., Pfeffer, W. T., M. S. Moussavi, M. S., and Abdalati. W.: Rapid
expansion of Greenland's low-permeability ice slabs. *Nature*, 573, 403–407, 2019.
- Matsuoka, K. and Naruse, R.: Mass balance features derived from a firn core at Hielo Patagonico Norte, South America,
Arctic, *Antarct. Alp. Res*, 31, 333–340, 1999.
- Moholdt, G., Nuth, C., Hagen, J. O. and Kohler, J.: Recent elevation changes of Svalbard glaciers derived from ICESat laser
455 altimetry. *Remote Sens. Environ.*, 114, 2756–2767, 2010a.
- Moholdt, G., Hagen, J. O., Eiken, T. and Schuler, T. V.: Geometric changes and mass balance of the Austfonna ice cap,
Svalbard. *The Cryosphere*, 4, 21–34, 2010b.
- Munneke, P. K., Ligtenberg, S. R. M., Van Den Broeke, M. R., Van Angelen, J. H. and Forster, R. R.: Explaining the
presence of perennial liquid water bodies in the firn of the Greenland Ice Sheet. *Geophys. Res. Lett.* 41, 476–483, 2014.
- 460 Oerter, H., Reinwarth, O., and Rufli, H.: Core drilling through a temperate Alpine glacier (Vernagtferner, Oetztal Alps) in
1979, *Zeitschrift für Gletscherkunde und Glazialgeologie*, 18, 1–11, 1982.
- Neff, P. D., Steig, Eric J., Clark, Douglas H., McConnell, Joseph R., Pettit, Erin C., and Menounos, Brian.: Ice-core net snow
accumulation and seasonal snow chemistry at a temperate-glacier site: Mount Waddington, southwest British Columbia,
Canada. *J. Glaciol.* 58(212), 1165–1175. <https://doi.org/10.3189/2012JoG12J078>, 2012.
- 465 Nuth, C., Moholdt, G., Kohler, J., Hagen, J. O., and Käab, A.: Svalbard glacier elevation changes and contribution to sea
level rise, *J. Geophys. Res.*, 115, F01008. <https://doi.org/10.1029/2008JF001223>, 2010.
- Pälli, A., Kohler, J. C., Isaksson, E., Moore, J. C., Pinglot, J. F., Pohjola, V. A., and Samuelsson, H.: Spatial and temporal
vari- ability of snow accumulation using ground-penetrating radar and ice cores on a Svalbard glacier, *J. Glaciol.*, 48, 417–
424, 2002.
- 470 Parry, V., Nienow, P., Mair, D., Scott, J., Hubbard, B., Steffen, K., and Wingham, D.: Investigations of meltwater refreezing
and density variations in the snowpack and firn within the percolation zone of the Greenland ice sheet. *Ann. Glaciol.* 61–68.
2007.
- Pelto, M., Kavanaugh, J., and McNeil, C.: Juneau Icefield Mass Balance Program 1946–2011, *Earth Syst. Sci. Data*, 5, 319–
330, <https://doi.org/10.5194/essd-5-319-2013>, 2013.
- 475 Pohjola, V. A., Moore, J. C., Isaksson, E., Jauhiainen, T., van de Wal, R. S. W., Martma, T., Meijer, H. A. J., and Vaikmäe,
R.: Effect of periodic melting on geochemical and isotopic signals in an ice core from Lomonosovfonna, Svalbard. *J.*
Geophys. Res., 107, 4036, 2002.
- Samimi, S. and Marshall, S. J.: Diurnal Cycles of Meltwater Percolation, Refreezing, and Drainage in the Supraglacial
Snowpack of Haig Glacier, Canadian Rocky Mountains. *Front. Earth Sci.* 5, 1–15. <https://doi.org/10.3389/feart.2017.00006>,
480 2017.
- Schneider, T.: Water movement in the firn of Storglaciären. *J. Glaciol.* 45, 286–294, 1999.



- Schneider, T. and Jansson, P.: Internal accumulation in firn and its significance for the mass balance of Storglaciären, Sweden, *J. Glaciol.*, 50, 25–34, 2004.
- Sharp, R. P.: Features of the firn on Upper Seward Glacier St. Elias Mountains, Canada, *J. Geol.*, 59, 599–621, 1951.
- 485 Shiraiwa, T., Koshima, S., Uemura, R., Yoshida, N., Matoba, S., Uetake., and Got, M. A.: High net accumulation rates at Campo de Hielo Patagonica Sur, South America, Revealed by analysis of 45.97m long ice core. *Ann. Glaciol.*, 35, 84–90, 2002.
- Trabant, D. C. and Mayo, L. R.: Estimation and effects of internal accumulation on five glaciers in Alaska. *Ann. Glaciol.*, 6, 113–117, 1985.
- 490 van As, D., Box, J. E., and Fausto, R. S.: Challenges of Quantifying Meltwater Retention in Snow and Firn: An Expert Elicitation., *Front. Earth Sci.* 4(101), [https://doi: 10.3389/feart.2016.00101](https://doi.org/10.3389/feart.2016.00101), 2016.
- Wagner, Philip W.: Description and evolution of snow and ice features and snow surface forms on the Kaskawulsh Glacier. *Icefield Ranges Research Reports*. 51-53, 1963.
- Williamson, S., Zdanowicz, C., Anslow, F., S. Clarke, G. K. C., Copland, L., Danby, R. K., Flowers, G. E., Holdsworth, G., 495 Jarosch, A. H., and Hik, D. S.: Evidence for elevation-dependent warming in the St. Elias Mountains, Yukon, Canada. *J. Clim.* 3253–3269, [https://doi:10.1175/jcli-d-19-0405.1](https://doi.org/10.1175/jcli-d-19-0405.1), 2020.
- Yalcin, K., Wake, C. P., Kreutz, K. J., and Whitlow, S. I.: A 1000-yr record of forest fire activity from Eclipse Icefield, Yukon, Canada. *The Holocene*, 16(2), 200–209, <https://doi.org/10.1191/0959683606hl920rp>, 2006.
- Zdanowicz, C., Smetny-Sowa, A., Fisher, D., Schaffer, N., Copland, L., Eley, J., and Dupont, F.: Summer melt rates on 500 Penny Ice Cap, Baffin Island: Past and recent trends and implications for regional climate, *J. Geophys. Res. Earth Surf*, 117, F02006, [https://doi:10.1029/2011JF002248](https://doi.org/10.1029/2011JF002248), 2012.
- Zdanowicz, C., Fisher, D., Bourgeois, J., Demuth, M., Sheng, J., Mayewski, P., Kreutz, K., Osterberg, E., Yalcin, K., Wake, C., Steig, E., Froese, D., and Goto-Azuma, K.: Ice Cores from the St. Elias Mountains, Yukon, Canada: Their Significance for Climate, *Atmospheric Composition and Volcanism in the North Pacific Region, Arctic*, 1–23, 2014.

505

510



515 **Table 1.** Ice content, bulk firn density (ρ_b) and background firn density (ρ_f) in each core. Firn density calculations omit the seasonal snowpack, i.e. reported depths represent meters from the top of the surface.

	Total Ice Content (m)	Total Ice Content (% vol)	ρ_b 4.4 -14 m (kg/m ³)	ρ_b 4.4 -21 m (kg/m ³)	ρ_b 4.4 -36 m (kg/m ³)	ρ_f 4.4 -14 m (kg/m ³)	ρ_f 4.4 -21 m (kg/m ³)	ρ_f 4.4 -36 m (kg/m ³)
Core 1	1.53	4.2	558	618	670	533	588	660
Core 2	0.82	3.8	518	599	na	na	na	na

520 **Table 2.** Positive degree days at Copland weather station from 2014 – 2018 with 2015 being the highest and 2014 the lowest. This was estimated from summer (JJA) hourly temperature data and a degree day melt factor of 3 mm w.e. (°C d⁻¹).

	2014	2015	2016	2017	2018	Average
PDD (°C d)	22	90	77	71	85	69
Melt (mm w.e.)	67	270	230	214	254	207
Mean Summer Temperature (JJA) °C	-2.8	-1.8	-1.0	-1.6	-1.6	-1.7
Mean Annual Temperature °C	-9.7	-9.6	-9.0	-10.6	-9.9	-9.8

Table 3. A selection of a variety of densities from firn around the world, modified from Huss (2013).

Reference	Location	Number of cores	Density (upper 10 m) (kg/m ³)	Accumulation rate (m w.e./yr)	Type
Ambach & Eisner (1966)	European Alps	1	700	1.2	Temperate
Oerter et al. (1982)	European Alps	3	600	~1	Temperate
Sharp (1951)	Western Canada	1	650	~1.5	Temperate
Zdanowicz et al., (2012)	Arctic Canada	2	560	0.3-0.6	Polythermal
Kreutz et al., (2001)	Tien Shan	1	650	1.3	Polythermal
He et al., (2002)	Himalaya	1	640	0.9	Polythermal
Matsuoka and	Patagonia	1	620	2.2	Temperate



Naruse (1999)					
Shiraiwa et al., (2002)	Patagonia	4	550	5-15	Temperate
Pälli et al., (2002)	Svalbard	1	510	0.4	Polythermal
Nuth et al., (2010)	Svalbard	3	510	~0.5	Polythermal
Sass and O'Neel (personal communication, February, 2019)	Alaska	1	669	1.5 - 2g	Temperate
This study	Western Canada (Kaskawulsh)	2	538	1.8	Temperate

525

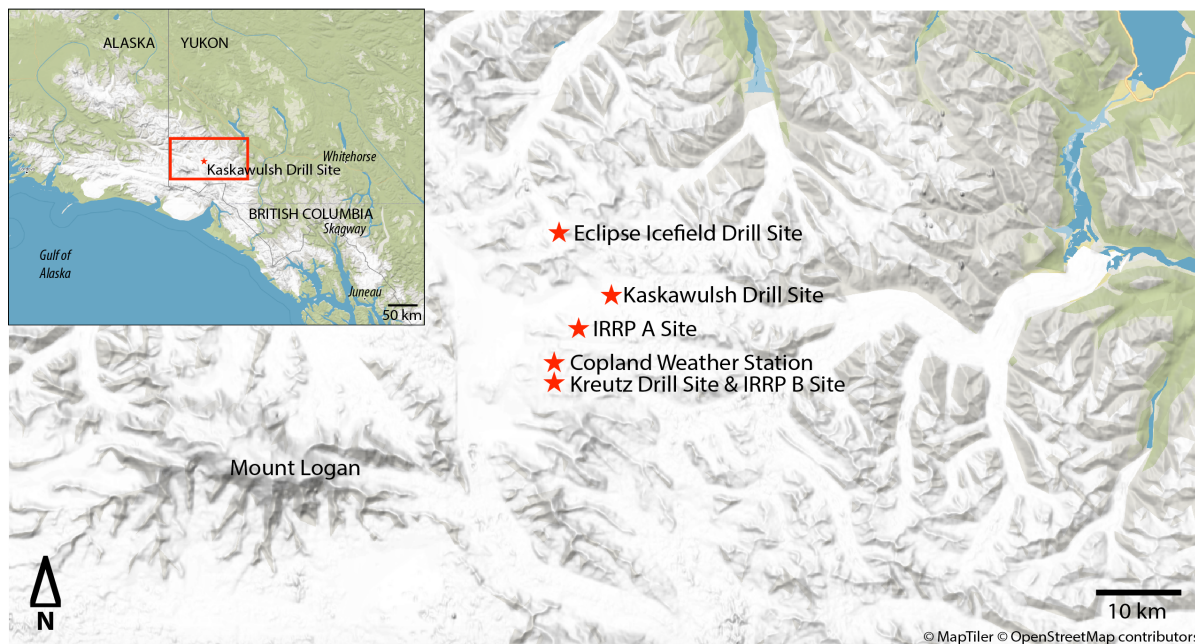
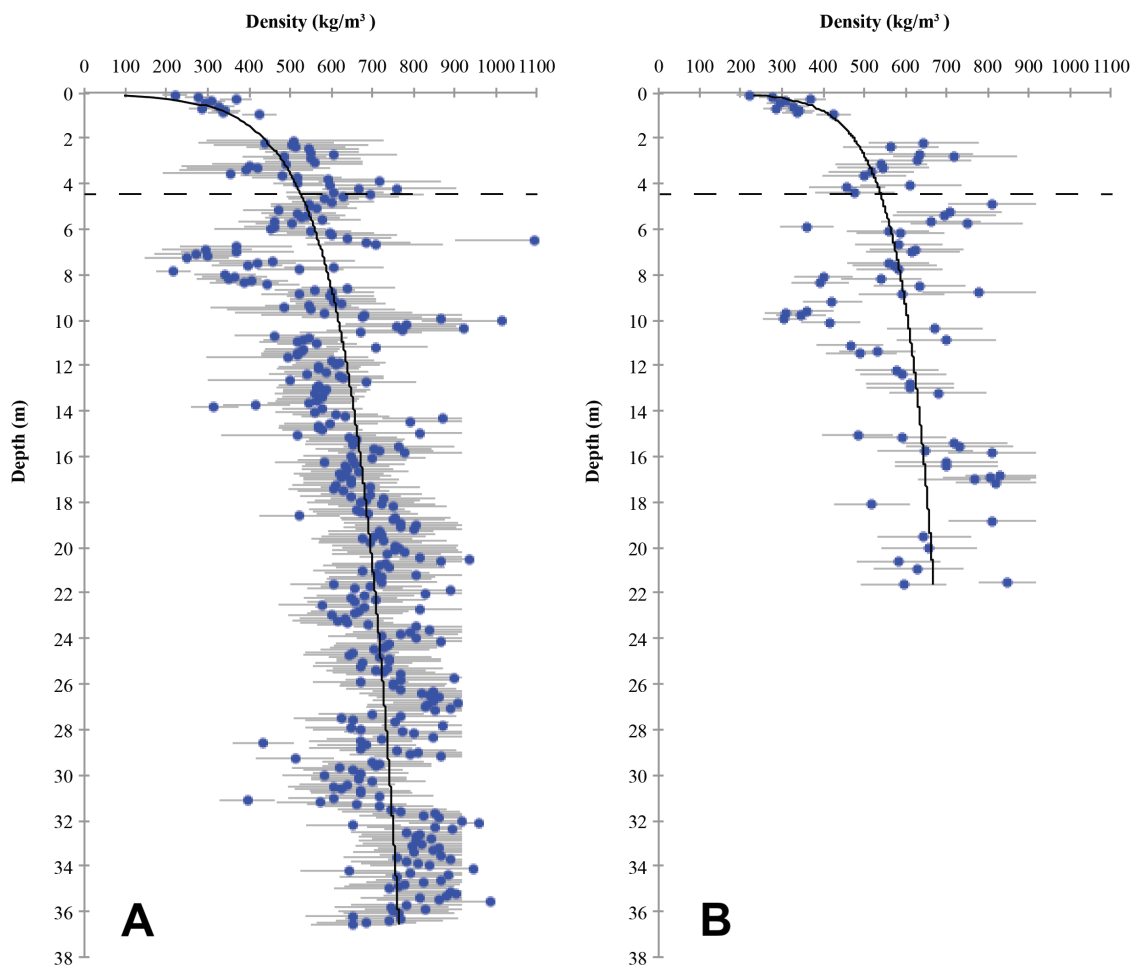
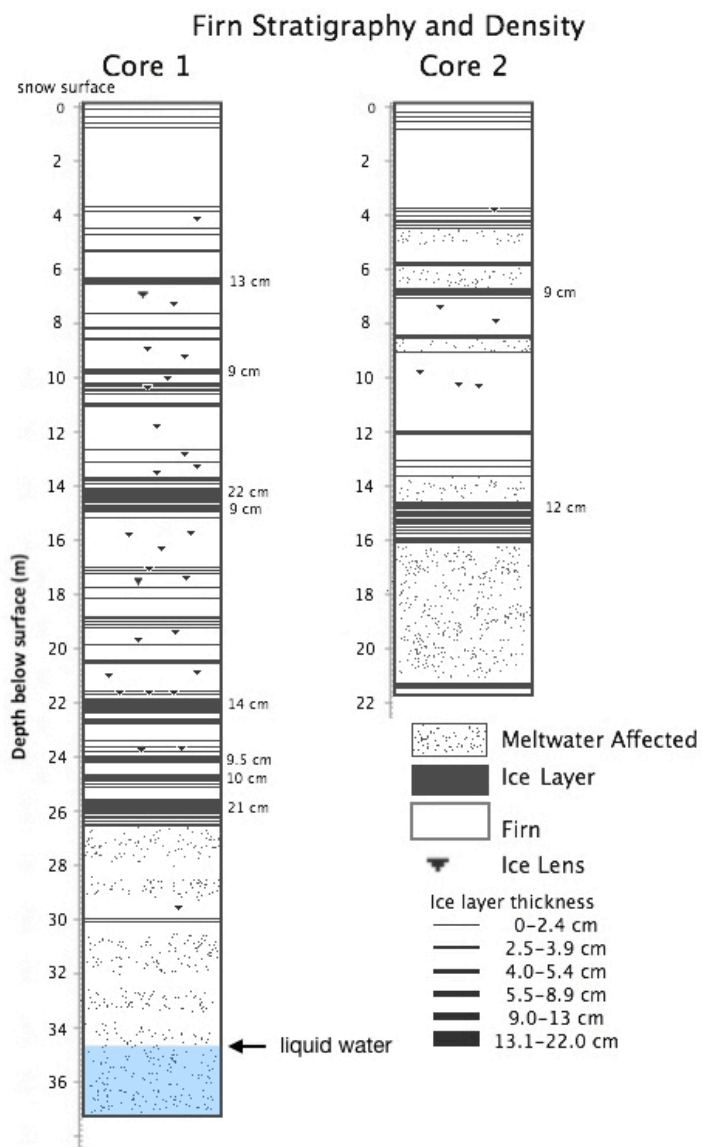


Figure 1: Notable locations in Kluane National Park: the 2018 Kaskawulsh Drill Site, Copland Weather Station, Kreuzt Drill site, Icefield Ranges Research Reports (IRRP) site A and B, and the Eclipse Icefield Drill Site. Maps made possible by <http://openmaptiles.org/>.

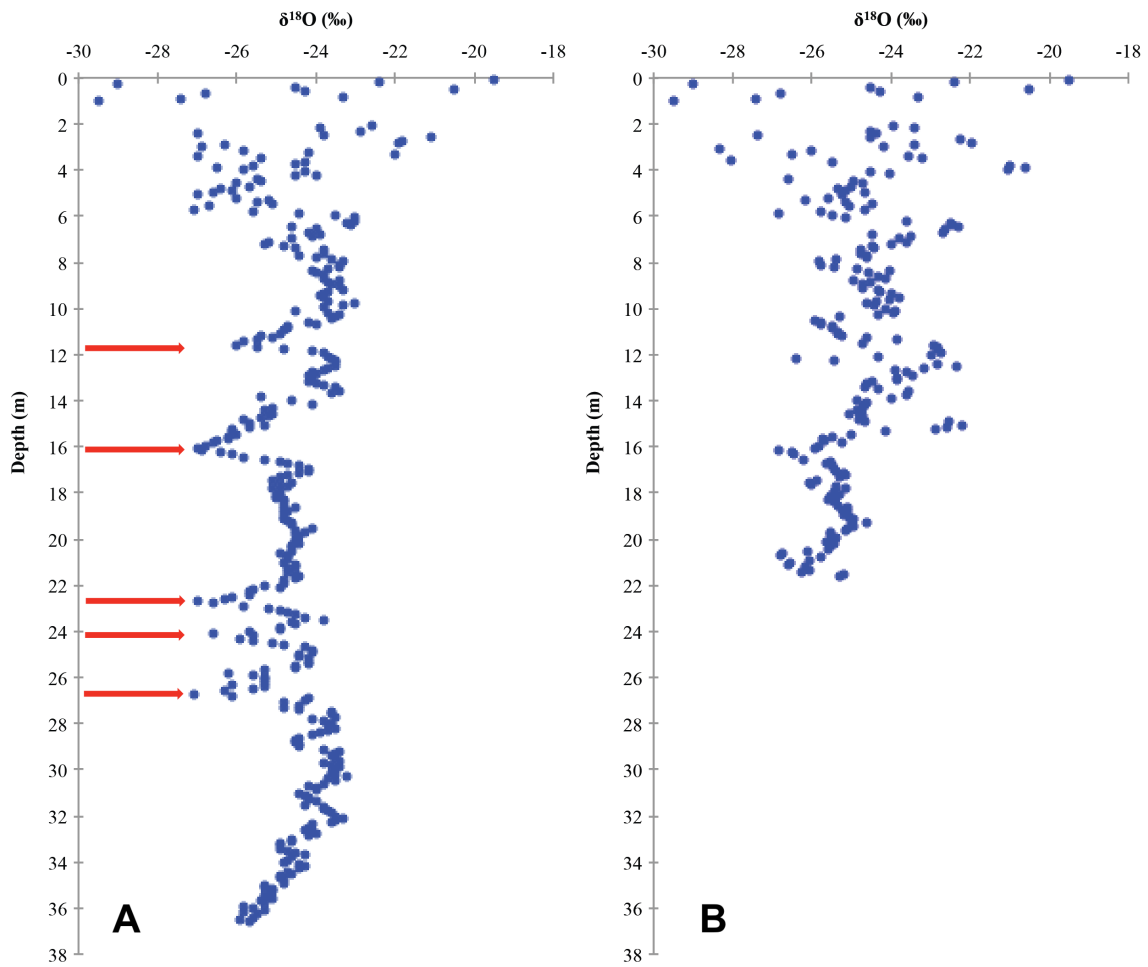


530

Figure 2: Measured densities of Core 1 (A) and 2 (B) with uncertainties and best-fit logarithmic curves (black line). The 0 references the snow surface. The first meter of data is from the snowpit. The depth of the 2017 summer horizon is indicated by the dashed line at 4.4 m.



535 **Figure 3: Firn core stratigraphy.** Ice layer thickness size was determined by distribution. Note that the ice layers in the first several meters of the core are interpreted as wind crusts. Differences in the cores are attributed to heterogeneous meltwater infiltration.



540

Figure 4: Stable oxygen isotope data, Core 1 (A) and Core 2 (B). The red arrows point to suggested winter peaks that have not been entirely washed out by the percolating melt water.